Non-adiabatic collisions in $H^+ + O_2$ system: An *ab initio* study

A SAIESWARI and SANJAY KUMAR*

Department of Chemistry, Indian Institute of Technology Madras, Chennai 600 036
e-mail: sanjay@iitm.ac.in

Abstract.   An *ab initio* study on the low-lying potential energy surfaces of $H^+ + O_2$ system for different orientations (γ) of H^+ have been undertaken employing the multi-reference configuration interaction (MRCI) method and Dunning's *cc-p*VTZ basis set to examine their role in influencing the collision dynamics. Nonadiabatic interactions have been analysed for the 2×2 case in two dimensions for $\gamma = 0°$, 45° and 90°, and the corresponding diabatic potential energy surfaces have been obtained using the diabatic wavefunctions and their CI coefficients. The characteristics of the collision dynamics have been analysed in terms of vibrational coupling matrix elements for both inelastic and charge transfer processes in the restricted geometries. The strengths of coupling matrix elements reflect the vibrational excitation patterns observed in the state-to-state beam experiments.

Keywords.   Ground electronic state; excited electronic state; potential energy surfaces; charge transfer.

1. Introduction

Proton interactions with molecules are of fundamental interest in nature. Proton-molecule systems constitute the prototype of ion–molecule reactions. In the interstellar space ion–molecule collisions occur dominantly leading to the formation of bound molecular ions. Many bound protonated species like H_3^+ N_2H^+, HCO^+, HCS^+, HCN^+, HO_2^+, etc. have been identified in the interstellar media through their radio-astronomical spectra.[1] On the other hand, the solar flare which mainly consists of protons can inject them into the Earth's atmosphere with a mean kinetic energy (KE) of 1–2 KeV.[2] The injected protons lose most of their KE by various inelastic processes and finally reach the stratosphere where they interact with several diatomic and polyatomic molecules in the collisions energy (E_{cm}) range 0–100 eV.

The interactions and the dynamics of collision energy transfer processes in proton–molecule systems have been the subject of both experimental and theoretical studies over the last few decades.[3] As a result, much more refined experimental data on vibrational-rotational excitations (including the charge-transfer (CT) processes) have become available for some of the systems. Effective vibrational-rotational excitations occur along with CT (if possible) processes in the

E_{cm} range of 0–30 eV. Molecular beam experiments coupled with proton energy-loss spectroscopy have been carried out with several diatomic molecules (H_2, N_2, O_2, CO, NO) and polyatomic molecules (CO_2, SF_6, CH_4).[3–7] These experimental results show an interesting selectivity for vibrational excitation, observed with apparently similar molecules. For example, the amount of vibrational excitation in N_2 is comparatively very low and is similar to that observed in CO and NO, but it is larger in H_2 and even larger in O_2, in a similar range of E_{cm}. One also observes certain mode selective vibrational excitation patterns in polyatomic molecules.[3]

Proton–molecule interactions operate over a wide range of distances. In the asymptotic limit the long range tail of the interaction potential becomes effective in terms of charge–polarizability and/or charge–dipole components, and at shorter distances the valence forces dominate the interactions. Being, electronically structureless, protons can penetrate the molecular electronic charge cloud deeply, and as a result, quite often the low-lying excited electronic states (ES) potential energy surface(s) (PES) shows (show) non-adiabatic interactions with the ground electronic state (GS) PES, thus influencing the dynamics of overall energy transfer processes.

A better theoretical understanding has become available for various systems over the years. For example, for the $H^+ + H_2$ system, an avoided crossing

*For correspondence

occurs between the GS PES and the ES PES which asymptotically correlates to the CT channel, the $H + H_2^+$.[3,8] The GS PES in the $H^+ + N_2$ system has been found to be well separated energetically from the low-lying ES PESs, but the ES PESs exhibit rich non-adiabatic interactions.[9] Exact quantum dynamical calculations for vibrational excitation processes in the vibrational close-coupling rotational infinite-order sudden approximation (VCC-RIOSA) framework[10,11] have been preformed using *ab initio* PESs for the $H^+ + H_2$ system[8] and the $H^+ + N_2$ system.[9] Recently, three-dimensional quantum mechanical calculations for the reactive and CT channels have also been carried out within the coupled states approximation for the $H^+ + H_2$ system,[12] and using the close-coupling formalism with hyper-spherical coordinates for the $D^+ + H_2$ system.[13] Using the later approach the details of quantum dynamics of the reactive CT has been analysed recently for the $H^+ + H_2$ system.[14] There exist an avoided crossing between the GS and the first ES PESs in the asymptotic regions for the $H^+ + CO$ system. Recently, a new full three-dimensional GS PES in Jacobi coordinates was obtained by our group[15] to study the time-independent quantum dynamics of vibrational excitations in the system in the framework of VCC-RIOSA scheme on the GS PES. Overall, the computed collision attributes were found to be in good agreement with the experiments. However, as many as three low-lying ES PESs are involved in the energy transfer processes in this system at $E_{cm} = 9.5$ eV.[16]

1.1 *Previous studies on $H^+ + O_2$ system*

Structured time-of-flight spectra of proton scattering from O_2 at scattering angles $5° \leq \theta_{cm} \leq 21°$ at $E_{cm} = 9.5$ eV show an anomalous vibrational excitation of O_2 molecule when compared with other diatomic targets like CO, N_2 and NO.[7] The transition probability for $(0 \rightarrow 1)$ for N_2, CO and NO increases with the scattering angle and reaches a maximum for O_2 in the region of 10°, while the transition probability for $(0 \rightarrow 2)$ has a maximum at 15° and it remains constant in the angular region between 15° and 20°.

The most detailed scattering data for CT in collisions of $H^+ + O_2$ was performed by Noll and Toennies in 1986.[17] They reported the H^+ and H atom time-of-flight distributions at $E_{cm} = 23.0$ eV for $\theta = 0°$ to 11°. The vibrational state resolved relative cross sections showed a weak rainbow maxima at

about 11° for inelastically scattered protons and two rainbow maxima at about $\theta = 1°$ and 10° for the H atom CT channel. Unfortunately, they could not find a complete satisfactory explanation for the comparatively large amount of vibrational energy transfer inferred from the proton time-of-flight spectra due to the lack of relevant potential energy surfaces during those times.

The adiabatic SCF potential energy curves for the title system in a restricted geometry was first examined by Staemmler and Gianturco[18] to understand the anomalous vibrational excitation in O_2 with proton collision energies of ~ 10.0 eV. An MRD-CI study on the electronic structure of the HO_2^+ molecule were done by Peyerimhoff and coworkers[19] which gave an insight in to the vertical ionization spectra and dissociation energies of the molecule. Sidis and coworkers proposed an effective model-potential approach in order to determine the potential energy surfaces and interactions relevant to the study of non-adiabatic proton–molecule collisions.[20] This method is based on the determination of matrix element of the electronic Hamiltonian in a basis of projected-valence-bond wave functions describing the incident state and excited state as well as charge transfer states generated by single orbital replacements from that state. They developed the essential diabatic states using two methods: (i) (M1) Configuration interaction calculations in orthogonal subspace and (ii) (M2) Rotation of adiabatic states achieving maximum overlap of the resulting states with strictly diabatic albeit crude prototypes. The two methods provide almost the same description of the surface crossing $R_c(r, \gamma)$ and associated interaction between the two diabatic charge exchange states except at those regions where the atom–molecule distance is smaller than R_c. Quantum mechanical calculations within the infinite order sudden approximation using these diabatic PESs and the coupling terms were able to reproduce the salient features of the experimental observations by Noll and Toennies.[21] The complex formation via translation-to-vibration energy exchange and the types of resonances exhibited by the complex were also studied using the same diabatic PES.[22]

Several low-lying potential energy surfaces for the $(HO_2)^+$ system obtained using the diatomics-in-molecules (DIM) approach and calibrated with *ab initio* data of Peyerimhoff and coworkers[19] have been generated by Schneider *et al* in 1988.[23] They were able to qualitatively reproduce the main features of the ground and lower excited states. The rotational exci-

tation using the rigid rotor and also within the IOS coupling scheme were studied on this system.[24] The computed results were in general agreement with some of the observed scattering features like rainbow positions and average rotational energy transfers.

In the $H^+ + O_2$ system there exists a direct curve crossing between the GS and the first ES PES in the collinear and perpendicular geometries. This becomes an avoided crossing for off-collinear approaches of H^+ and thus constitutes a conical intersection between the respective potential energy sufaces[25] in the full-dimensional nuclear configuration space. The curve crossing is located slightly farther out from the GS interaction well and towards the asymptotic region.[7,26] The non-adiabatic coupling terms between the two involved PES were computed analysed[26] and a three-dimensional quantum mechanical study of vibrational, state-resolved differential cross sections (DCS) for the direct inelastic and for the charge transfer scattering channel has been carried out using the semi empirical DIM PES.[27] The state-to-state DCS are found to follow closely the behaviour of the experimental quantities, both in the inelastic and the charge transfer channels. The vibrational energy was overestimated in the inelastic channel while in the charge transfer channel the same energy was underestimated by the calculations. The total flux distributions and the angular distributions were also reasonably well reproduced. However, the relative probability of the vibrational excitation channels and the vibronic charge transfer channels were at variance with experiments. On the other hand, the multiple ionization cross sections have been measured with H^+, D^+ and He^+ impact on N_2, O_2, CO and NO molecules in a collision energy range 50–300 KeV.[28]

1.2 *Present focus*

The purpose of the present study is to examine the role of the low-lying excited electronic states obtained using *ab initio* calculations, in influencing the overall dynamics of $H^+ + O_2$ collisions relevant to proton energy-loss experiments in the collision energy range $E_{cm} = 9.5$–30 eV. At these collision energies the experiment reveal large amount of inelastic vibrational excitations of O_2. We first analyse the behaviour of potential energy curves (PEC) of the ground electronic and low-lying electronic states as a function of R with the NO nuclear distance r fixed at its equilibrium value (theoretically determined at

MRCI/*cc-p*VTZ level), $r_{eq} = 2.293 \ a_0$, (r_{eq} (expt) $= 2.286 \ a_0$) for different angular approaches of H^+.
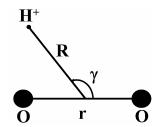
Although some information on the non-adiabatic interactions between the first two electronic states has become available in the literature, a detailed insight into the title system through the *ab initio* approach is still lacking. Hence, the present focus is to construct the relevant quasi diabatic potential energy surfaces and to gain insight into the non-adiabatic collisions. Also, we assume that only the GS and the first excited state PESs are involved in the dynamics. Nevertheless, at this collision energy the involvement of the second excited state cannot be ruled out as one observes non-adiabatic interactions between the first and second excited states at closer approach of H^+, where the latter state becomes accessible energetically. We have generated the vibrational coupling matrix elements for the elastic/inelastic and charge transfer processes for $\gamma = 0°$, 45° and 90°.

The paper is organized as follows. In §2 the details of the *ab initio* computations, quasi diabatic PECs and PESs are given. In §3, the characteristics of the vibrational coupling matrix elements for both inelastic and charge transfer channels are discussed. A summary with conclusion is given in §4.

2. Computation details

2.1 *Ab initio adiabatic potential energy curves and surfaces*

Ab initio calculations have been carried out in the Jacobi coordinates as shown in figure 1, where R is the distance of H^+ from the centre of mass of O_2, r is the interatomic distance of O_2 and $\gamma = \cos^{-1}(Rr)$. The calculations have been carried out in various molecular orientations, which are classified as, (i) H^+ approaching the oxygen atom in the collinear configuration ($\gamma = 0°$), (ii) H^+ approaching the centre of mass of the O_2 at a perpendicular orientation
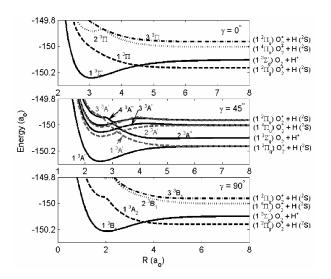

Figure 1. Jacobi Coordinates, r: Internuclear distance of NO, R: Distance of H^+ from centre of mass of NO and γ: $\cos^{-1}(R.r)$.

$\gamma = 90°$, and (iii) H^+ approaching the centre of mass of the O_2 molecule in any other configurations, $0° < \gamma < 90°$.

The computations have been performed in the C_{2v} (collinear and perpendicular) and C_s point groups (off-collinear). PECs as a function of R have been obtained for various molecular orientations with the set of grid points: $R = 1.4–7.0$ (0.2) a_0 and $7.0–15.0$ (1.0) a_0 for collinear approach, and $R = 0.2–7.0$ (0.2) a_0 and $7.0–15.0$ (1.0) a_0 for off-collinear and perpendicular approaches. The numbers in parentheses indicate the increment in the stated intervals. The adiabatic PECs of the ground- and the low-lying excited triplet states are obtained by the Multi-Reference Configuration interaction (MRCI) method using the MOLPRO software.[29,30] We have employed Dunning's cc-pVTZ basis sets for H and O atoms.[31]

The adiabatic PECs for $\gamma = 0°$, 45° and 90° as a function of R are shown in figure 2. For the collinear and perpendicular orientations ($\gamma = 0°$ and $\gamma = 90°$ in figure 2) there exist a direct curve crossing at $R = 4.54$ a_0 and $R = 3.61$ a_0, respectively, between the GS and the first ES leading to an exoergic CT channel, where the GS ($1\ ^3\Sigma^-/1\ ^3B_1$) corresponds to the entrance channel, O_2 ($1\ ^3\Sigma_g^-$) + H^+ and the excited state ($1\ ^3\Pi/1\ ^3A_2$) corresponds to the first CT channel, O_2^+ ($1\ ^2\Pi_g$) + H (^2S). This direct curve crossing occurs because there exist no coupling between the $\Sigma - \Pi$ symmetry (and $A_2 - B_1$ symmetry). The immediate next excited states correspond to the second and

Figure 2. Adiabatic potential energy curves for $\gamma = 0°$, 45° and 90° molecular orientation as a function of R. (r fixed at $r_{eq} = 2.293\ a_0$).

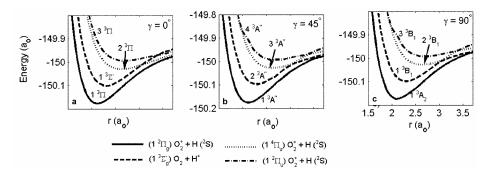third CT channels, O_2^+ ($1\ ^4\Pi_u$) + H(^2S) and O_2^+ ($1\ ^2\Pi_u$) + H (^2S), respectively, as denoted in figure 2.

These crossing regions becomes avoided crossings for the off-collinear geometries ($\gamma = 45°$ in figure 2) where the degeneracy in the Π symmetry is lifted and thus coupling between the ground ($1\ ^3A''$) and the first ES ($2\ ^3A''$) becomes a prominent factor. This is clearly illustrated in figure 2 for $\gamma = 45°$, where the GS corresponds to the first CT channel and the ES corresponds to the entrance channel as mentioned above. The degeneracy of the second and the third CT channels which also belongs to the Π symmetry in the collinear approach, is also lifted into A′ and A″ as shown in figure 2.
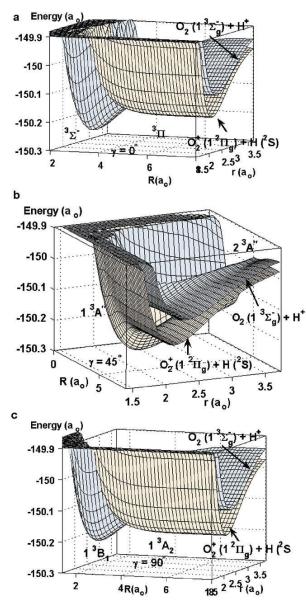
The adiabatic PECs for the same three orientations as shown in figure 2, but as a function of r (internuclear distance of the diatom) are shown in figure 3. In figure 3a the entrance channel ($1\ ^3\Sigma_g^-$) O_2 + H^+ crosses with the second and third CT channels at $r = 3.08$ a_0 and $r = 3.41$ a_0, respectively, for $\gamma = 0°$ due to the symmetry of the molecule. But for $\gamma = 45°$ (figure 3b) and $\gamma = 90°$ (figure 3c), these crossings turn out as avoided crossing regions since all the states belong to the same symmetry $^3A''$ for $\gamma = 45°$ and $^3B_1$ for $\gamma = 90°$. From figures 2 and 3, it is evident that the system shows several avoided crossings along R as well as along the r coordinates. Most of these avoided crossings are actually cuts through conical intersections of the potential energy surfaces, and they approximately exhibit a Landau–Zener type of coupling.[32] (e.g. between the ground ($1^3A''$) and the first excited ($2\ ^3A''$) states along the R coordinate). Hence for the collision energy in the range of $E_{cm} = 9.5–30$ eV, these excited states are expected to influence the dynamics of the system. For dynamics calculation we focus on the PESs for the $1\ ^3A''$ and $2\ ^3A''$ states and their radial coupling in the $\gamma = 45°$ approach of H^+. The adiabatic PESs for the ground and the first excited states as a function of R and r are shown in figure 4 for $\gamma = 0°$, 45° and 90°. The PESs for $\gamma = 0°$ and 90° crosses along a line, where as the PES for $\gamma = 45°$ shows avoided crossing. The labels of the PESs are given inside the figure.

2.2 *Diabatization*

For computational convenience, we treat the coupling between the pair of electronic states involved in a diabatic representation where the nuclear kinetic energy operator $\hat{T}$ is diagonal and potential energy

Figure 3. Adiabatic potential energy curves for $\gamma = 0°$, 45° and 90° molecular orientations as a function of r. (R fixed at 15 a_0).

Figure 4. The lowest two adiabatic PESs for $\gamma = 0°$, 45° and 90° molecular orientations as function of R and r.

operator $\hat{V}$ is non-diagonal. In contrast, in the adiabatic representation, the former is non-diagonal and the latter is diagonal. The diabatization procedures, their exactness and their associated advantages for numerical computations have been discussed and documented in the literature in detail.[33–48] A general discussion on it has been recently published.[44] The diabatization procedure is described below.

2.2a   *Two-state coupling:* In the adiabtic electronic states kinetic coupling matrix elements are of the form,

$$\left\langle \psi_m^a \left| \frac{\partial^l}{\partial R^l} \right| \psi_n^a \right\rangle, \tag{1}$$

where $l = 1$ or 2. The terms with $l = 2$ are generally smaller in magnitude, and therefore not included in the dynamical calculations.[33] For the present study we also assume that they will have negligible effect on the dynamics. The kets, $|\psi_m^a\rangle$ and $|\psi_n^a\rangle$, represent the electronic wavefunctions of the two involved adiabatic states and R stands for the radial nuclear coordinates. Non-adiabatic coupling matrix elements (NACME) have been computed between the coupled states by numerical differentiation using the finite difference method.[49]

$$\left\langle \psi_m^a \left| \frac{\partial}{\partial R} \right| \psi_n^a \right\rangle$$

$$= \frac{1}{2\Delta R} \langle \psi_m^a (R_0 + \Delta R) | \psi_n^a (R_0 - \Delta R) \rangle, \tag{2}$$

where ΔR is a small increment. We have used MOLPRO[29] to compute the NACME values. In this procedure first the orbitals are determined at the reference geometry, then the calculations are per-

formed at the displaced geometries. The NACME values have been obtained using the MRCI method by computing the finite-differences of CI wavefunctions with $\Delta R = 0.0002 a_0$. Additional calculations were also performed for a few data points with $\Delta R = 0.002 a_0$ and the obtained values were identical with the values obtained with $\Delta R = 0.0002 a_0$. In earlier non-adiabatic studies for He–CN collisions[50] and for H_2S photodissociation,[51,52] NACME values were also computed using the MOLPRO software with similar increments in ΔR.

For the two-state coupling, the transformation from an adiabatic representation, with electronic wavefunctions ψ_m^a, $m = 1, 2$, to a diabatic representation characterized by the electronic wavefunctions ψ_m^d, $m = 1, 2$, is achieved by the unitary transformations,

$$\begin{pmatrix} \psi_1^d \\ \psi_2^d \end{pmatrix} = \begin{pmatrix} \cos\alpha & \sin\alpha \\ -\sin\alpha & \cos\alpha \end{pmatrix} \begin{pmatrix} \psi_1^a \\ \psi_2^a \end{pmatrix}, \qquad (3)$$

where α is the mixing-angle describing the mixing between the two adiabatic electronic states and is a function of R. Using (3), the matrix elements of $\hat{H}_{el}$ in the diabatic representation are given by,

$$V_{11}^d = \langle \psi_1^d | \hat{H}_{el} | \psi_1^d \rangle = V_1^a \cos^2\alpha + V_2^a \sin^2\alpha \qquad (4)$$

$$V_{22}^d = \langle \psi_2^d | \hat{H}_{el} | \psi_2^d \rangle = V_1^a \sin^2\alpha + V_2^a \cos^2\alpha \qquad (5)$$

$$V_{12}^d = \langle \psi_1^d | \hat{H}_{el} | \psi_2^d \rangle = (V_1^a - V_2^a) \cos\alpha \sin\alpha \qquad (6)$$

where $\psi_{1,2}^d$ are the electronic wavefunction of the two coupled states in the diabatic representation and their corresponding potential values are given by V_{11}^d and V_{22}^d. $V_{1,2}^a$ are the potential energy values in the adiabatic representation whose corresponding electronic wavefunctions are give by $\psi_{1,2}^a$. The coupling between the two state is given by V_{12}^d and $V_{12}^d = V_{21}^d$.
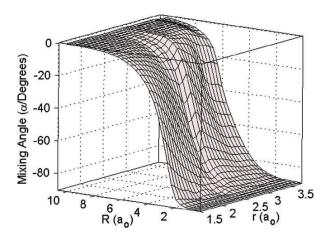
Other approximate methods[48,49,52–55] have also been suggested which avoid the direct computation of NACME and where α is obtained from the CI coefficients of the electronic wavefunctions. For example, Heumann *et al*[51] used the CI coefficients to achieve diabatization for the photodissociation study of H_2S. Later Simah *et al*[52] suggested and improved this scheme by determining the diabatic wavefunction (and the corresponding CI vectors) so that they vary as little as possible as a function of geometry. This condition is met by using the invariance of the MRCI energies with respect to unitary transformation among the active orbitals so that the geometry dependence of the orbitals is minimized. This is accomplished by maximizing the overlap for all the pairs of active orbitals at R_{ref} with those at neighbourhood geometry R' using the Jacobi rotation technique. The description of the procedure for a general $(n \times n)$ case is given in the Ref. 52 along with the application for the photodissociation of H_2S. This procedure has been incorporated in the MOLPRO software. It is worth pointing out that Balint–Kurti *et al* (see Ref. 45) have used this scheme in producing the five lowest diabatic PECs for O_3 system. In the present study we have obtained the quasidiabatic states directly by determining the diabatic wavefunctions using the MOLPRO software.

We have computed the NACME values between the $1\ ^3A''$ and $2\ ^3A''$ states as a function of R and parametrically dependent on r. The mixing angle is also obtained for the two-state case directly from the MOLPRO software using the CI coefficients. The mixing angle has a sigmoidal nature as one goes from small R to large R values. A two-dimensional view of the mixing angle for $\gamma = 45°$ is shown in figure 5. The value of the mixing angle varies from $\pi/2$ to $0°$ with increase in R coordinate which clearly indicates the change in the electronic wavefunction character at the avoided crossing region. Once the mixing angle is known as a function of R, the diabatic potential matrix defined in (4)–(6) can be obtained. The quasidiabatic potential matrix elements have also been obtained directly from the MOLPRO software with $R_{\text{ref}} = 15.0\ a_0$. The quasidiabatic potential surface for $\gamma = 45°$ are given in figure 6a and they clearly show a crossing seam around $R \approx 4.0\ a_0$. The coupling between these two states is also given in figure 6b. The coupling potential gradually dies to zero at a larger value of R.
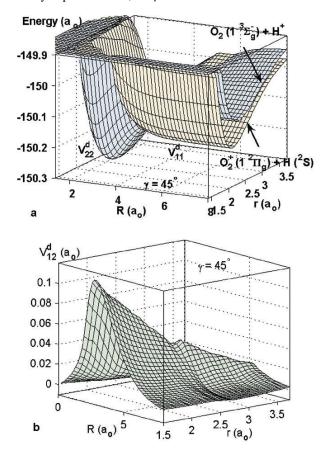
3. Vibrational coupling matrix elements

At such collision energies the rotational motion and the translational motion can be decoupled, which leads to drastic simplification of the decoupling of the angular momenta. In the vibrational close-coupling rotational infinite-order sudden approximations (VCC–RIOSA) the radial Schrödinger equation for the restricted approach is given by

$$\left[\frac{d^2}{dR^2} - \frac{l(l+1)}{R^2} + k_{ij}^2 \right] \Xi_{ij}(R) =$$

$$2\mu_{ABC} \sum_{i'} \sum_{j'} V_{i',j',ij}(R,\gamma) \Xi_{i',j'}(R), \qquad (7)$$

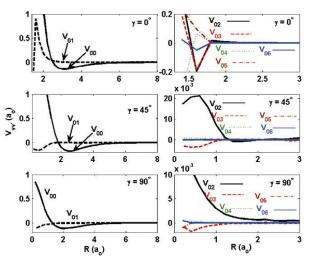**Figure 5.** Mixing angle as a function of R and parametrically dependent on r, for $\gamma = 45°$.

Figure 6. (**a**) Quasidiabatic PESs and coupling potential as a function of R and parametrically dependent on r, for $\gamma = 45°$. (**b**) The diabatic coupling potential V_{12}^d as a function of R and r.

with $k_{ij}^2 = 2\mu_{ABC}(E - \varepsilon_j^i)$

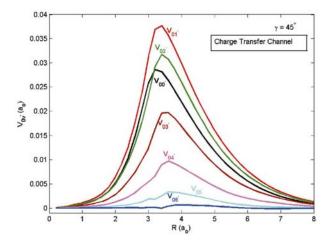$$V_{i'j',ij}(R,\gamma) = \langle \phi_{j'}(r) | V_{i',i}(R,r,\gamma) | \langle \phi_j(r) \rangle$$

$$V_{i',j}(R,r,\gamma) =$$

$$\langle \psi_{ei'}(R,r,q) | \hat{V}(R,r,\gamma,q) | \langle \psi_{ei}(R,r,q) \rangle$$

In this framework, the quantum transition probabilities crucially depend on the nature of the vibrational coupling matrix elements $V_{vv'} = \langle \phi_v(r) | V_{in}(R,r,\gamma) | \phi_{v'}(r) \rangle$, where, ϕ_v denotes the asymptotic vibrational wavefunction of the target for the vibrational state v which is considered as the initial state or the entrance channel. $\phi_{v'}$ denotes the asymptotic vibrational wavefunction of the final state or the exit channel for the vibrational wavefunction v' and V_{in} is the $H^+ + O_2$ interaction potential. To illustrate their behaviour, the diagonal matrix elements, V_{00} (elastic channel) and non-diagonal matrix elements, $V_{0v'}$ (inelastic channel), are shown in figure 7 as a function of R for $\gamma = 0°$, $45°$ and $90°$. From figure 7 it is clear that both diagonal (elastic channel) V_{00} and the off-diagonal (inelastic channel) $V_{0v'}$ show a rather smooth behaviour as a function of R. The elastic channel V_{00} exhibits a deep attractive well for all the three approaches of H^+ and therefore they are likely to couple strongly with the translational mode over a wide range of R values. Also, it is stronger for $\gamma = 45°$ as compared to other approaches.

In contrast, the inelastic element V_{01} shows a very weak coupling when compared to the V_{00} element and they are effective only at very short values of R. The strength of V_{01} decreases in going from $\gamma = 0°$ to $90°$. The other inelastic elements like V_{02}, V_{03}, V_{04}, V_{05}, V_{06} also show the same trend. The magnitude of

Figure 7. Vibrational coupling matrix elements for the elastic V_{00} and inelastic $V_{0v'}$ as a function of R.

Figure 8. Vibrational coupling matrix elements for the charge transfer channel $V_{0v'}$ as a function of R.

these inelastic elements other than V_{00} and V_{01} for any particular γ value are in comparable limits. The vibrational coupling elements for higher v (like $v' \geq 7$ and above) are very small in magnitude and hence were not included in the plot. Hence, the minimum number of vibrational states in the inelastic channel that has a significant contribution in the dynamical quantities are $v' = 6$. This suggests that the vibrational inelasticity would be rather high for this system which is in accordance with the experimental observation of Krutein and Linder.[5] The experimentally observed differential cross section (DCS)[17] also shows a similar kind of behaviour for the inelastic process.

The matrix element $V_{00'}$, $V_{01'}$ (CT channel) are shown in figure 8. The matrix elements $V_{01'}$ and $V_{02'}$ show a stronger coupling than that of $V_{00'}$ element. This is also reflected in the experimentally observed DCS by Noll and Toennies.[17] Moreover, at least for $v' \leq 6$, there exist a strong coupling after which these charge transfer coupling matrix elements are negligibly small and hence are not included in the figure 8. Thus the vibrational inelasticity in the charge transfer system, that is, O_2^+ is also expected to be high.

4. Summary

Ab initio calculations on the $H^+ + O_2$ system have been carried out in restricted approaches of H^+ ($\gamma = 0°$, 45° and 90°) at the MRCI/*cc-p*VTZ level of theory using the Dunning's basis set. The adiabatic as well as diabatic PESs for the GS and the first ES

were obtained using the MOLPRO software. Vibrational coupling matrix elements, which are the crucial quantities in a time-independent quantum mechanical calculations, were also computed. Their strength and characteristics reflected as a function of radial coordinate R qualitatively reflect the correct behaviour of experimentally observed state-to-state transition probability and DCS for vibrational excitation for both the inelastic and the charge transfer channels. It will be worthwhile to obtain the full three-dimensional surfaces for both the GS and ES to carry out the quantum mechanical calculations and compare the results with the experiments. Such a study is currently under process.

References

1. Herbst E 2001 *Chem. Soc.* **30** 168
2. Klemperer W 1970 *Nature* (*London*) **227** 1230
3. Niedner-Schatteburg G and Toennies J P 1992 *Adv. Chem. Phys.* **LXXXII** 553
4. Udseth H, Giese C F, Gentry W R 1974 *J. Chem. Phys.* **60** 3051
5. Krutein J and Linder F 1979 *J. Chem. Phys.* **71** 559
6. Niedner-Schatteburg G, Dissertation, Georg-August-Universität Göttingen, Fachbereich Physik 1988 Also published as Bericht 13/1988 Max-planck-institut für Strömungsforschung, Göttingen 1988
7. Gianturco F A, Gierz U and Toennies 1981 *J. Phys. B: At. Mol. Phys.* **14** 667
8. Schinke R 1980 *J. Chem. Phys.* **72** 3916; Baer M, Niedner-Schatteburg G and Toennies J P 1989 *J. Chem. Phys.* **91** 4196; Gianturco F A and Kumar S 1995 *Chem. Phys.* **196** 485; Gianturco F A and Kumar S 1995 *J. Chem. Phys.* **103** 2940
9. Gianturco F A, Kumar S and Schneider F 1996 *Chem. Phys.* **211** 33; Gianturco F A, Kumar S, Ritschel T, Vetter R and Zulicke L 1997 *J. Chem. Phys.* **107** 6634
10. Schinke R and McGuire P 1978 *Chem. Phys.* **31** 391; Parker G and Pack R T 1978 *J. Chem. Phys.* **72** 1585
11. Gianturco F A, 1979 *The transfer of molecular energies by collisions* (Berlin: Springer)
12. Last I, Gilibert M and Baer M 1997 *J. Chem. Phys* **107** 1451
13. Takayanagi T, Kurosaki Y and Ichihara A 2000 *J. Chem. Phys.* **112** 2615

14. Ushakov V G, Nobusada K and Osherov V I 2001 *Phys. Chem. Chem. Phys.* **3** 63
15. Dhilip Kumar T J and Kumar S 2004 *J. Chem. Phys.* **121** 191
16. Dhilip Kumar T J, Saieswari A and Kumar S 2006 *J. Chem. Phys.* **124** 034314
17. Noll M and Toennies J P 1986 *J. Chem. Phys.* **85** 3313
18. Staemmler V and Gianturco F A 1985 *Int. J. Quant. Chem.* **XXVIII** 553
19. Vazquez G J, Buenker R J and Peyerimhoff S D 1986 *Mol. Phys.* **59** 291
20. Grimbert D, Lassier-Givers B and Sidis V 1988 *Chem. Phys.* **124** 187
21. Sidis V, Grimbert D, Sizun M and Baer M 1989 *Chem. Phys. Lett.* **163** 19
22. Grimbert D, Sidis V and Sizun M 1994 *Chem. Phys. Lett.* **230** 47
23. Schneider F, Zülicke L, DiGuacomo F, Gianturco F A, Paidarová I and Polák R 1988 *Chem. Phys.* **128** 311
24. Gianturco F A, Palma A and Schneider F 1989 *Chem. Phys.* **137** 177
25. Domcke S, Yarkony D R and Köppel H 2004 *Conical intersections: Electronic structure, dynamics and spectroscopy* (Singapore: World scientific)
26. Gianturco F A, Palma A and Schineider F 1990 *Int. J. Quant. Chem.* **XXXVII** 729
27. Gianturco F A, Palma A, Semprini E, Stefani F and Baer M 1990 *Phys. Rev.* **A42** 3926
28. Siegmann B, Werner U, Kaliman Z, Roller-Lutz Z, Kabachnik N M and Lutz H O 1989 *Phys. Rev.* **A66** 052701
29. MOLPRO is a package of *ab-initio* programs written by Werner H-J, Knowles P J, Schütz M, Lindh R, Celani P, Korona T, Rauhut G, Manby F R, Amos R D, Bernhardsson A, Berning A, Cooper D L, Deegan K J O, Dobbyn A J, Eckert F, Hampel C, Hetzer G, Lloyd A W, McNicholas S J, Meyer W, Mura M E, Nickla*β* A, Palmieri P, Pitzer R, Schumann U, Stoll H, Stone A J, Tarroni R and Thorsteinsson T. Dunning Jr. T H 1989 *J. Chem. Phys.* **90** 1007
30. Dunning T H Jr 1989 *J. Chem. Phys.* **90** 1007
31. Zener C 1932 *Proc. R. Soc. London.* **A137** 696; Landau L D 1932 *Phys. X. Sowjetunion* **2** 46; Stuckelberg E C G 1932 *Helv. Phys. Acta.* **5** 369; Litchen W 1963 *Phys. Rev.* **131** 229; Nikitin E E 1968 *Theory of non-adiabtic transitions. Recent developments of the landau–Zener-(linear) model, Chemische Elementarprozesses* (ed.) H Hartmann (Berlin: Springer-Verlag) 43; Rosen N and Zener C 1932 *Phys. Rev.* **40** 502; Child M S 1971 *Mol. Phys.* **20** 171
32. Mead A and Truhlar D 1982 *J. Chem. Phys.* **77** 6090
33. Smith F T 1969 *Phys. Rev.* **179** 111
34. Baer M 2002 *Adv. Chem. Phys.* **124** 39; Baer M 2002 *Phys. Rev.* **358** 75; Baer M 1985 *Theory of chemical reaction dynamics* (ed.) M Baer (Boca Raton: CRC FL) chapter 4, vol. II
35. Baer M, Schatteberg G N and Toennies J P 1989 *J. Chem. Phys.* **91** 4169
36. Sidis V 1992 *Adv. Chem. Phys.* **82** 73
37. Pacher T, Cederbaum L S and Köppel H 1993 *Adv. Chem. Phys.* **84** 293
38. Schinke R 1993 *Photodissociation dynamics* (Cambridge: Cambridge University Press)
39. Nakamura H 1996 *Dynamics of molecules and chemical reactions* (eds) R E Wyatt and J Z H Zhang (New York, Marcel Dekker)
40. Child M S 2002 *Adv. Chem. Phys.* **124** 1; Adhikari S and Billing G D 2002 *Adv. Chem. Phys.* **124** 143; Worth G A and Robb M A 2002 *Adv. Chem. Phys.* **124** 355
41. Jasper A W, Zhu C, Nagia S and Truhlar D G 2004 *Faraday Discuss.* **127** 1
42. Köppel H 2004 *Faraday Discuss.* **127** 35
43. Baer M, Vertesi T, Halasz G J, Vibok A and Suhai S 2004 *Faraday Discuss.* **127** 337
44. General discussion 2004 *Faraday Discuss.* **127** 81
45. Baragan P, Errea L F, Macias A, Mendez L, Rabadan I, Riera A, Lucas J M and Aguilar A 2004 *J. Chem. Phys.* **121** 11629; Romero T, Aguilar A and Gadea F X 1999 *J. Chem. Phys.* **110** 6219
46. Vertesi T, Bene E, Vibok A, Halasz G J and Baer M 2005 *J. Phys. Chem.* **A109** 3476 and references therein.
47. Top Z H and Baer M 1977 *Chem. Phys.* **25** 1; Baer M and Beswick J A 1979 *Phys. Rev.* **A19** 1559; Baer M 1983 *Molecular collision dynamics* (ed.) J M Bowman (Heidelberg: Springer, Berlin)
48. Werner H-J and Meyer W 1981 *J. Chem. Phys.* **74** 5802
49. Werner H-J, Follmeg B and Alexander M H 1988 *J. Chem. Phys.* **89** 3139; Werner H-J, Follmeg B, Alexander M H and Lemoine P 1989 *J. Chem. Phys.* **91** 5425
50. Heumann B, Weide K, Duren R and Schinke R 1998 *J. Chem. Phys.* **98** 5508 and references therein
51. Simah D, Hartke B and Werner H-J 1999 *J. Chem. Phys.* **111** 4523 and references therein
52. Köppel H, Domcke W and Cederbaum L S 1984 *Adv. Chem. Phys.* **57** 59
53. Desouter-Lecomte M, Deharebg D and Lorquet J C 1987 *J. Chem. Phys.* **86** 1429
54. Pacher T, Cederbaum L S and Köppel H 1988 *J. Chem. Phys.* **89** 7367
55. Petrongolo C, Hirsch G and Buenker R J 1990 *Mol. Phys.* **70** 825; Hirsch G, Buenker R J and Petrongolo C 1990 *Mol. Phys.* **70** 835